온도민감형 Poly(acrylamide-co-N-isopropyl acrylamide) 수화젤의 합성, 분석 그리고 흡습성

Şeyda Taşar[†] and Ramazan Orhan

Department of Chemical Engineering, Firat University

(2019년 9월 16일 접수, 2019년 11월 2일 수정, 2019년 11월 21일 채택)

Temperature-responsive Poly(acrylamide-co-N-isopropyl acrylamide) Hydrogel: Synthesis, Characterization, and Sorption Application

Şeyda Taşar[†] and Ramazan Orhan

Department of Chemical Engineering, Firat University, 23279, Elazig, Turkey
(Received September 16, 2019; Revised November 2, 2019; Accepted November 21, 2019)

Abstract: Acrylamide-based hydrogels were used to remove cationic Basic Blue 3 (BB3) dye from aqueous solutions, in this study. First, acrylamide-based hydrogel was synthesized and characterized using SEM, FTIR and swelling analysis. The effects of various parameters were investigated to determine the removal of the BB3 dye from aqueous solutions. The sorption yield of BB3 dye of the hydrogel was determined to be 99%. The desorption efficiency was found to be above 90%. The sorption experimental data were evaluated using applying the Langmuir, Freundlich, Temkin, and Dubinin-Radushkevich (D-R) isotherm models. It was determined that the Langmuir was more suitable for isotherm the process. The maximum sorption capacity was calculated as 28.3 mg/g. Pseudo first order, pseudo second order, intraparticle diffusion, and Endovich kinetic models were used to calculate the kinetic parameters. It was concluded that the pseudo second-order kinetic model was described by the adsorption data very well.

Keywords: hydrogel, swelling ratios, sorption, kinetic and thermodynamic evaluation.

Introduction

Various dyestuffs and pigments are used for coloring various industrial products, such as textile products, plastics, carpets, papers, printings, cosmetics, and foods.[1-4] The dye and textile industries are among the most polluting sectors, and they produce the most toxic waste among all of the industrial sectors. Approximately 10-15% of the dyestuffs used in textile industries is contained in the effluent, resulting in the production of significant amounts of wastewater. The spreading of this wastewater into the environment results in the coloration of water, limited oxygenation capacity, and decreased photosynthetic activities in water environments as a result of decreased penetration by sunlight, which lead to chronic and acute poisoning.[1,2] Also the wastewater can cause serious human health issues, including hypersensitive reactions, geno-

toxic effects, and carcinogenic effects.[2,5]

The dyestuffs, which are commercially available in many varieties, are classified in various ways, according to the structure, color, and methods of application. Generally, dyes are classified as anionic (reactive, acid and direct dyes), cationic (all basic dyes) and non-ionic (disperse dyes) dyestuffs according to the particle load they produce during their dissolution in the aqueous medium food.[1-3] Cationic dyes, which are used extensively in the paint industry, also are used in the textile industry, especially for the dyeing of acrylic fibers.[3] Cationic dyes, which interact with the negatively-charged surfaces of cell membranes, enter cells, and accumulate in the cytoplasm, are known to be more toxic than anionic dyes. Due to their intended use, the dyestuffs have a low biodegradation rate and are resistant to environmental conditions.[1,6] Therefore, the wastewater that contains these dyes must be treated before being released into the environment.[4] However, cationic dyes cannot be removed completely by conventional treatment methods, such as physical methods (coagulation, irradiation, ion exchange, membrane separation), chemical methods

[†]To whom correspondence should be addressed.
sydtasar@hotmail.com; sydtasar@firat.edu.tr
ORCID 0000-0003-3184-1542

(chemical oxidation, degradation, electrochemical destruction), and biological treatment methods.[1-5,7,8] In addition, the toxic effects of the secondary components that result from the degradation of paint pose risks to the environment. In treating wastewater that contains dyestuffs, the sorption process is generally more preferred over other removal processes. Because sorption process has important advantages. The design of sorption process is simple, has a low installation cost, is easy to use and has low sensitivity to toxic substances.[1,5,7]

Several studies have been conducted on the sorption of various cationic dyes on various adsorbent materials.[9-28] But, as is known from published research papers, the molecular structure of the adsorbate in a sorption process and its related properties (e.g., molecular size and shape, polar character, hydrophobic character, ionic or nonionic, ionic load centers number and type) directly affect the sorption yield and the capacity of the adsorbent.[2,3,5] Therefore, the sorption behaviors of dye molecules may be different depending on their different molecular structures, sorption amount, sorption kinetics, and thermodynamics.[3,5] Thus, work must be done to determine the sorption yield and capacity for each dye molecule and adsorbent pair.

Hydrogels are cross-linked polymeric structures with hydrophilic character.[29-32] They do not dissolve in water, and they can take a large amount of water into their structures and swell.[30-34] Hydrogels can be sensitive to various environmental factors, such as temperature, pH, electric and magnetic fields, and ionic strength, and they react to changes in these factors by changes in their volumes that are reversible. The water sorption behavior of hydrogels is one of the most important factors that determine their properties and areas of usage. The hydrogel structure in contact with water passes from the glassy form to the rubber form with the swelling. Because of this ability to change and their high water-holding capacity, hydrogels are used in agriculture, the production of hygienic products, tissue engineering, controlled drug release, separation processes, and wastewater treatment.[31,33,34] Gels, which are hydrophilic and also known as polyelectrolytes, are prepared from monomers that contain hydrophilic groups and are water-ionizing. The hydrophilicity of gels generally is known to increase with the presence of water-soluble groups, such as -OH, -COOH, -CONH$_2$, -SO$_3$H.[30,31] In addition, sorption in hydrogels usually is due to the presence of the ionizable functional groups of the monomers that form hydrogels. These functional groups have a complex forming role in the removal of dye molecules from wastewater.[32] Recently, hydrogels have been used extensively for the preparation of membranes and sorbents in water purification and separation.[29-39]

In this study, acrylamide(AAm)-based hydrogels were synthesized using chemical polymerization and characterized by instrumental analysis methods. And the structural and morphological properties before and after the sorption process of hydrogel employed as a sorbent in the experiments were defined using SEM and FTIR analysis. The temperature-dependent equilibrium swelling ratios of hydrophilic gels were determined with gravimetric methods in water. Also, they were used as a sorbent for the removal of BB3 dye from aqueous solutions. Various parameters that are effective in the removal of dyes, i.e., hydrogel composition, initial pH, contact time, temperature, and initial dye concentration were examined to determine their effects on sorption efficiency and sorbent capacity. In addition, the sorption mechanism was analyzed using various kinetic models and thermodynamic models. The desorption efficiency of hydrogels was investigated.

Experimental

Materials. We purchased the following chemical compounds from Sigma-Aldrich (USA). Acrylamide [CH$_2$=CHCONH$_2$, AAm (99%)], *N*-isopropyl acrylamide [(H$_2$C=CHCONHCH(CH$_3$)$_2$, NIPAm (≥99%)], *N,N,N,N* tetramethylethylenediamine [(CH$_3$)$_2$NCH$_2$CH$_2$N(CH$_3$)$_2$, TEMED (99%)], ethylene glycol dimethacrylate [CH$_2$=C(CH$_3$)COOCH$_2$CH$_2$-OCOC(CH$_3$)=CH$_2$, EGDM (98%)], ammonium persulfate [(NH$_4$)$_2$S$_2$O$_8$, APS (98%)].

The chemicals used in the synthesis process were used without further purification. All of the supplied chemicals are either analytical grade or highest purity.

Synthesis of Hydrogels. The AAm-based hydrogels were synthesized in solution medium according to the free radical polymerization mechanism. The multi-functional cross-linking agent ethylene glycol dimethacrylate (EGDM) was used in the preparation of the polymeric gels. To synthesize the AAm *co*-NIPAm polymeric gels, the calculated amount (x g) of AAm monomer was dissolved in 1 mL of distilled water using a magnetic stirrer. The calculated amount (1-x) of NIPAm comonomer were added to the reaction mixture and dissolved completely. The total amount of the monomers that was used in the synthesis was kept constant at one gram, and calculations were made using this amount. Then, we added 0.25 mL/0.013 mmol of EGDM, followed by the addition of 0.2 mL/0.044 mmol of APS as the initiator and the addition of 0.25 mL/0.017 mmol TEMED solution (% 1) as the accel-

erator. The prepared reaction mixture was placed in 2 mL glass pipettes and placed in an oven at 60±1 ℃. At the end of the polymerization, the glass pipettes were broken carefully, and the polymeric gels were removed from the pipettes. The gels were sliced thicknesses of 0.5 cm and placed in distilled water. Any unreacted monomers and reactants were removed by washing for 48 h. Before the gels were used for the water sorption and dye sorption experiments, the gel samples were dried at 60±1 ℃ in an oven.

The compositions of the hydrogels that were synthesized are provided in Table S1.

Analyses and Characterization Studies. The structural properties before and after the sorption process of hydrogel employed as a sorbent in the experiments were defined using a Shimadzu IRSpirit Fourier transform infrared spectrophotometer (FTIR). To reveal the surface morphology of networked polymeric gel before and after the adsorption process, SEM analysis was performed using the ZEISS scanning electron microscope. Before SEM analysis, all of the hydrogel samples were coated with gold.

During the experiments, pH measurements were performed with a Thermo Scientific Orion 1112000 3-star pH meter. Spectrophotometric measurements were conducted using a Bausch & Lomb Spectronic 20 UV/vis spectrophotometer. Weighing operations were done with an Ohaus brand Analytical Plus model balance with ± 0.0001 grams sensitivity.

Determination of Water Sorption Capacities. The swelling of the synthesized polymeric gels was characterized using applying dynamic swelling tests to the cross-linked polymeric samples at 25, 35, 45, and 55 ℃. The AAm-based polymeric gel in the dry state was weighed with a precision of 0.0001 g,

placed in a beaker with distilled water at a constant temperature, and allowed to swell. The moment the polymeric gel entered the water was taken as $t = 0$, and the polymeric gels were removed from the water at certain time intervals and it weighed. The weighing process was continued regularly until constant weights were obtained over time. At the end of the dynamic swelling tests, graphs depicting the percentage of swelling as a function of time were prepared, and inflatable isotherms were formed. It was observed that the percentage swelling values calculated using the help of eq. (1) of the polymeric samples eventually reached a stable equilibrium. This constant value is expressed as the equilibrium water absorption capacity $(S_e)(g_{water}/g_{gel})$ of the hydrogels, and it is calculated as follows:

$$S_e = \frac{W_{wet} - W_{dry}}{w_{wet}} \qquad (1)$$

where; S_e is the equilibrium water absorption capacity, and W_{wet} and W_{dry} are the weight of swollen and dried hydrogel samples, respectively. Dynamic swelling experiments were performed in three replicates, and the averages of the data were presented.

Preparation of Colored Wastewater. Basic dye Basic Blue 3 (BB3, dye content: 25%, λ_{max}: 654 nm, molecular weight: 359.89) was supplied from Sigma-Aldrich (USA). The chemical structure of BB3 was given in Figure S1. The stock solution of BB3 dye was prepared with a concentration of 1000 mg/L. All of the working solutions and dilutions were prepared using distilled water.

Determination of Dye Sorption Capacities. The effect of gel composition (crosslinker ratio and comonomer ratio), ini-
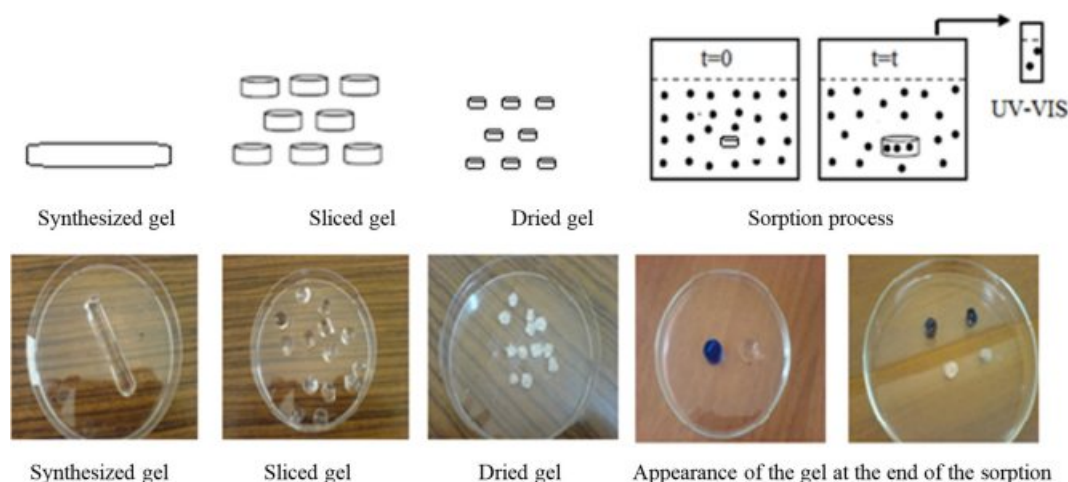
Figure 1. Schematic representation of the dye sorption process.

Table 1. Effects of the Parameters and Their Working Ranges

Variable Parameters	Unit	Value
Co-monomer ratio of hydrogel	NIPAm/Monomer (w/w:g/g)	1/10 - 2/5 - 1/4 - 2/7 - 2/5
Cross linker ratio of hydrogel	EGDM/Monomer (v/w:ml/g)	0/1 - 1/5 - 2/5 - 3/5 - 4/5
Initial pH of dye solution	pH	1.5 - 2.5 - 3.5 - 4.5 - 5.5 - 6.5 - 8.5 - 10.5
Temperature of solution	K	298 - 308 - 318 - 328
Initial concentration of dye solution	ppm (mg/L)	50 - 60 - 70 - 80 - 100

tial pH, temperature and dye concentration were investigated in sorption experiments that were conducted at a constant agitation rate in a temperature-controlled, shaking water bath. Figure 1 shows a schematic representation of the sorption process of the BB3 dye molecules. Table 1 summarizes the effects of the parameters and the study intervals.

Samples were analyzed at specific time intervals during the sorption period, and the concentration of dye remaining in solution was measured spectrophotometrically at the wavelength, $\lambda_{max} = 654$ nm, using a Bausch & Lomb Spectronic 20 UV/vis spectrophotometer. The sorption process continued until equilibrium was reached. The sorption capacity (q_e) and the sorption efficiency (Y_a) of the hydrogel based on the experimental conditions were calculated using eq. (2) and eq. (3), respectively:

$$q_e = \frac{V x (C_0 - C_e)}{m} \tag{2}$$

$$Y_a(\%) = \frac{(C_0 - C_t)}{C_0} \times 100 \tag{3}$$

where m (g) is the mass of the hydrogel; V (L) is the volume of the aqueous medium; $C_0, C_e,$ and C_t are the initial, equilibrium, and final concentrations of the BB3 dye molecules in the aqueous medium, respectively; and q_e is the equilibrium sorption capacity, which represents the amount of BB3 dye molecules adsorbed by the activated peanut shells (in mg/gm) at equilibrium conditions.

Kinetic and Thermodynamic Analysis of the Sorption Process. To better understand the mechanisms of sorption and to design a sorption system, the capacity of sorption and the mechanism of sorption must be evaluated. The structure of the sorption process was elucidated and calculated kinetic and thermodynamic parameters by analyzing the obtained experimental data in five different kinetic models and in four different isotherm models. Kinetic and thermodynamic model equations used in the study were presented in Table 2 and Table S3. The kinetic and isotherm studies were investigated

using the gels that were prepared for the NIPAm/monomer ratio of 0/1, the EGDM/monomer ratio of 1/4.

Determination of Desorption Efficiency. The desorption studies were investigated using the gels that were obtained as a result of isotherm studies. After the sorption experiments, the BB3 dye molecules-loaded hydrogel particles were collected from the solutions. The hydrogels were then washed with 0.1 M HCl solution using magnetic stirring for 24 h. The washing solution was renewed every 4 h. And the dye solutions obtained after washing were collected in a glass vial to determine the concentration. The collected dye solution concentration (C_s) was determined and desorption efficiency was calculated using eq. (4) and eq. (5).

$$D_e(\%) = \frac{(C_a - C_s)}{C_a} \times 100 \tag{4}$$

$$C_a = C_0 - C_t \tag{5}$$

where C_a is the BB3 concentrations which were sorbed from hydrogel at the equilibrium, and C_s is the BB3 concentration of washing solution which was obtained desorption process.

Results and Discussion

Water Sorption Capacity of Hydrogel. It is well known that the ability of the polymers to swell depends on their chemical structures, the solvent, the molar mass of the polymer, the elasticity of the polymer chain, the cross-linking density of the network, the hydrophilic character of polymeric network, the heterogeneity of the chemical structure of the polymeric chain, and the temperature of the solvent. Thus, in this study, we examined the effect of the temperature of the solvent, the crosslinking density of the hydrogel, and the hydrophilicity of the gel on the equilibrium swelling ratio. Table 2 shows the effect of these parameters on the equilibrium swelling ratio.

The experimental results indicated that the water sorption capacity of the gel decreased as the ratio of the co-monomer of

Table 2. Equilibrium Water Sorption Capacity of Hydrogel

Variable parameters	Range of value	Equilibrium water sorption capacity (S_e) (g_{water}/g_{gel})
Variable: Co-monomer ratio of hydrogel	0/1	12.93
NIPAm/Monomer (w/w:g/g)	1/5	10.96
Temperature:298 K	2/5	8.652
EGDM/Monomer (v/w:mL/g):1/4	3/5	5.251
	4/5	4.261
Variable: Cross-linking ratio of hydrogel	1/10	4.160
EGDM/Monomer (v/w:mL/g)	2/5	9.908
Temperature: 298 K	1/4	12.93
NIPAm/Monomer(w/w:g/g):0/1	2/7	10.25
	2/5	5.061
Variable: Temperature of water (K)	298	12.93
NIPAm/Monomer(w/w:g/g):0/1	308	13.99
EGDM/Monomer (v/w:mL/g):1/4	318	5.055
	328	4.661

the hydrogel (NIPAm/monomer (w/w: g/g)) increased because the hydrophilicity of the gel was decreased. The highest swelling ratio (12.9 g_{water}/g_{gel}) was achieved in the sorption experiment in which the gel was synthesized with the NIPAm/monomer ratio of 0/1. Therefore, the effect of cross-linking density on the equilibrium swelling ratio was investigated using gels that were prepared using preserving that ratio.

Until the cross-linking density reaches the EGDM/monomer (v/w: mL/g) ratio of 0.25/1, the potential swelling ratio of the gel increased from 4.16 to 12.9 g_{water}/g_{gel} as the cross-linking density of the gel was increased. However, after this critical value, the increase in the cross-link density led to a decrease in the water sorption capacity. This occurred because cross-linking above the critical value caused the gel to lose its elasticity and to form a fragile structure. Therefore, the effect of the temperature of the solvent on the equilibrium swelling ratio was investigated using gels that were prepared using the critical cross-linker ratio.

Generally, it is well known that the swelling ratio of polymer networks may increase or decrease as the temperature increases. The temperature at which the AAm-based gel films absorbed the maximum amount of water was determined to be 308 K. It was observed that the water sorption capacity of the gel at this temperature was about 14 g_{water}/g_{gel}. As the temperature of the solution increased and exceeded 308 K, the water sorption capacity of the gel decreased significantly because the gel tended to shrink. It was determined that the swelling rate of the gel decreased to 4.7 g_{water}/g_{gel} at 328 K.

The equilibrium swelling ratios of the hydrogels that were synthesized were compared with values available in the literature. It was observed that the degree of swelling of the AAm-based gel that we synthesized was somewhat lower than was reported in the literature. This result occurred because the gels that we synthesized had higher cross-linking densities than the gels reported in the literature.

Removal Yield of BB3 Dye Molecules. Effect of the co-Monomer Ratio: To investigate the effect of the co-monomer ratio, i.e., hydrogel NIPAm/monomer (w/w: g/g), on the sorption process, sorption experiments were conducted in which the ratio was varied from 0/1 to 4/5 g/g, while other experimental conditions were kept constant. Figure 2 shows the sorption curves that were obtained, and, when these curves were examined, it was apparent that the sorption yield of the dye molecules and the sorbent capacity of hydrogel decreased as the co-monomer ratio that was used in the synthesis of the hydrogel increased. When the ratio was increased from 0/1 to 4/5, the removal yield decreased from about 99% to 34%, and the sorption capacity decreased from about 17.3 to 6.4 mg/g after 1440 min. Therefore, the effect of cross-linking density on the sorption yield was investigated using the gels that were prepared using preserving the NIPAm/monomer ratio of 0/1.

Effect of the Cross-linker Ratio: In order to evaluate the effect of the cross-linker ratio on the sorption process, we conducted sorption experiments using varying the cross-linker ratio of hydrogel EGDM/monomer (v/w: mL/g) from 1/10 to 2/5 mL/g while keeping the other experimental conditions con-
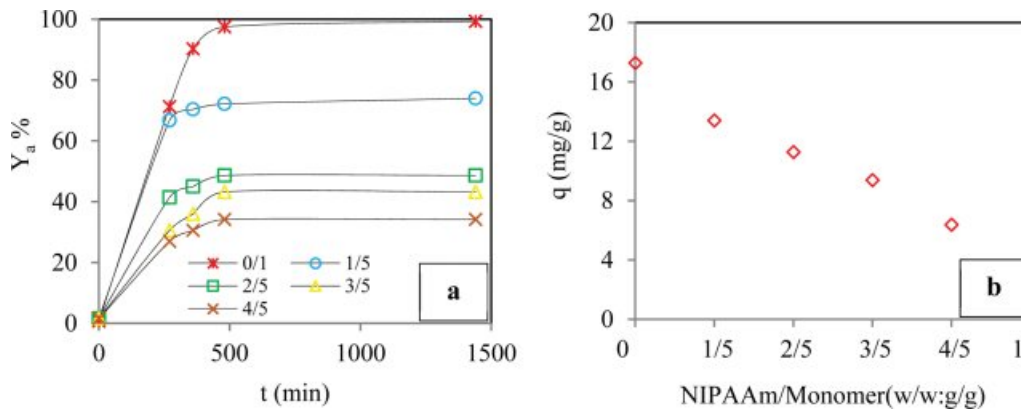
Figure 2. Effect of the co-monomer ratio on adsorption yield of dye (a); adsorption capacity of dye (b) (Conditions: pH of 6.5; temperature of 298 K; dye conc. of 50 ppm; contact time of 1440 min; agitation rate 180 rpm; cross-linker ratio of 1/4 mL/g; co-monomer ratio of 0/1 - 4/5 g/g).
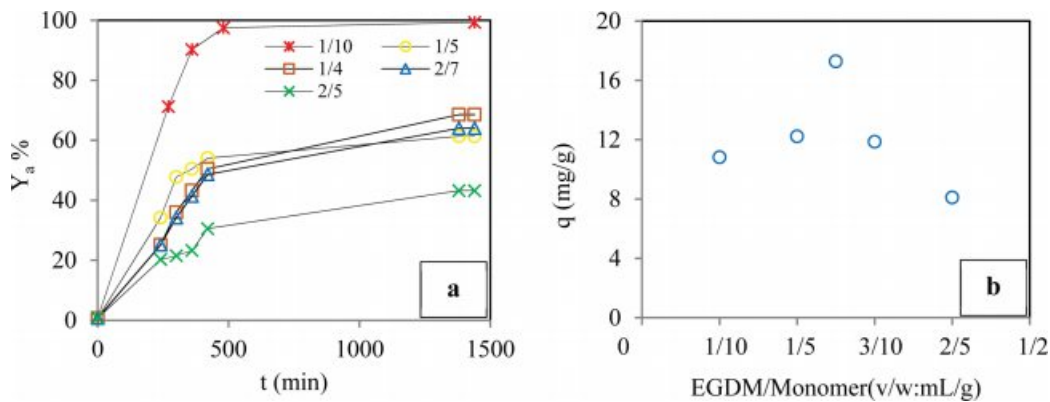
Figure 3. Effect of the cross-linker ratio on adsorption yield of dye (a); adsorption capacity of dye (b) (Conditions: pH of 6.5; temperature of 298 K; dye conc. of 50 ppm; contact time of 1440 min; agitation rate 180 rpm; cross-linker ratio of 1/10-2/5 mL/g; co-monomer ratio of 0/1 g/g).

stant. Figure 3 shows that the removal efficiency of the BB3 molecules was increased from about 61% to 93% by increasing the cross-linking dose to 1/4 mL/g at 1/10 mL/g. However, at higher cross-linker ratios above 1/4 (mL/g), significant reductions in the sorption yields were determined due to a decrease in the swelling capacity of the gel. A similar trend was observed for the sorption capacity. These results showed that the cross-linker ratio of 1/4 (mL/g) was sufficient to achieve maximum sorption yield for the experimental conditions we used. Therefore, the effects of other sorption parameters on the sorption yield were investigated using the gels that were prepared using preserving the EGDM/monomer ratio of 1/4.

Effect of the Initial pH of Aqueous Medium: The acidity of the initial solution is among the most important factors that affect the sorption of dye molecules. The effect of pH on the

sorption of BB3 molecules by AAm-based hydrogel was investigated in the pH range of 1.5 to 10.5 while keeping the other experimental conditions constant. Figure 4 shows that the sorption capacity of the gel increased in the pH range of 1.5 to 6.5, and it reached its maximum value (17.3 mg/g) at a pH value of 6.5. When the pH exceeded 6.5, a rapid decrease in sorption capacity occurred as a result of the decrease in the degree of ionization of the functional groups of the gel.

Effect of Contact Time and the Temperature of the Solution: Kinetic evaluation experiments were performed at four different temperatures, i.e., 298, 308, 318, and 328 K, to investigate the effect of temperature on BB3 sorption when other experimental conditions were kept constant. Examination of the sorption curves in Figure 5 shows that the dye removal efficiency and adsorbent capacity decreased as the temperature increased. When the temperature was increased from 298 K to
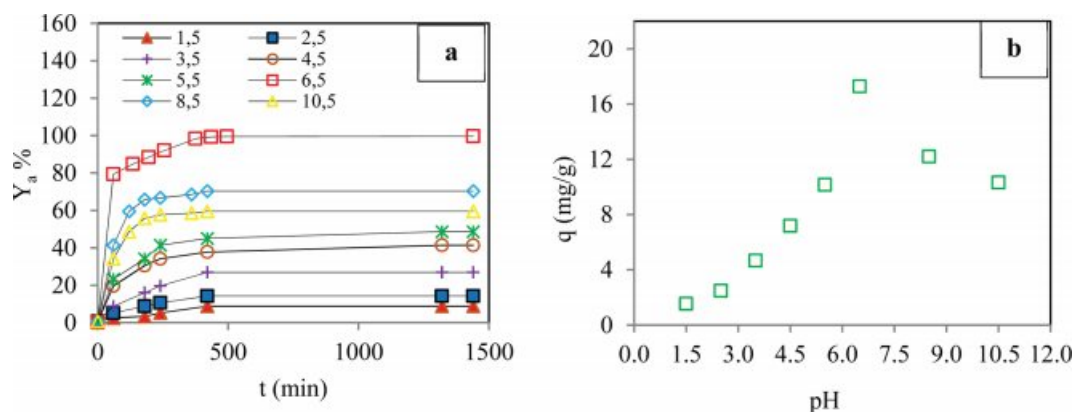
Figure 4. Effect of the initial pH of the aqueous medium on adsorption yield of dye (a); adsorption capacity of dye (b) (Conditions: pH of 1.5-10.5; temperature of 298 K; dye conc. of 50 ppm; contact time of 1440 min; agitation rate 180 rpm; cross-linker ratio of 1/4 mL/g; co-monomer ratio of 0/1 g/g).
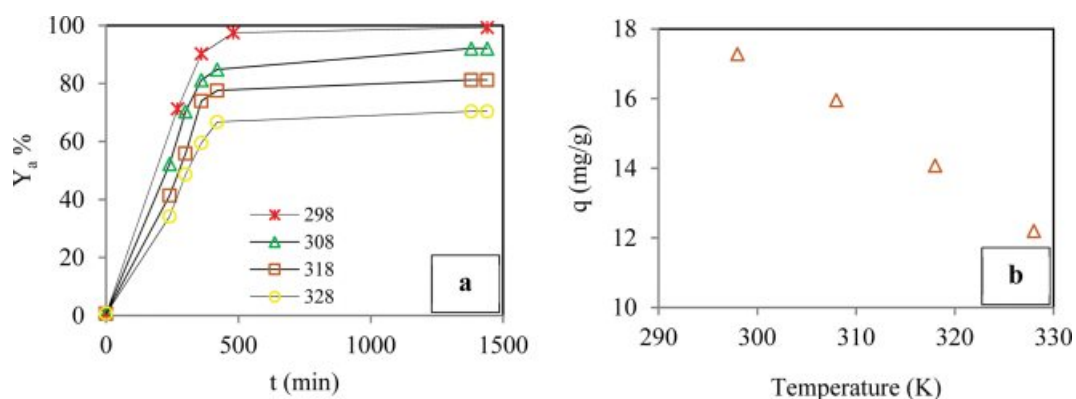
Figure 5. Effect of the temperature on adsorption yield of dye (a); adsorption capacity of dye (b) (Conditions: pH of 6.5; temperature of 298-328 K; dye conc. of 50 ppm; contact time of 1440 min; agitation rate 180 rpm; cross-linker ratio of 1/4 mL/g; co-monomer ratio of 0/1g/g).

328 K, the removal yield decreased from about 99.3% to 66.7%, and the sorption capacity decreased from about 17.3 to 12.2 mg/g after 420 min. It was observed that the increase in the contact time resulted in increased removal of the dye molecules. As a result, in the studies that were conducted at 298 K, the highest removal efficiency, i.e., 99.3%, was attained at the end of the 440 min sorption period. Extension of the contact time beyond 440 min did not have an important effect on the yield of the removal. Therefore, it was concluded that the optimum contact time and temperature were 440 min and 298 K, respectively, given the exothermic nature of the sorption of BB3 dye molecules.

Effect of the Initial Concentration of Dye Molecules: Figure 6 shows that the removal yield of BB3 dye molecules was reduced as the initial concentration of the dye was increased. In contrast, the sorption capacity of the hydrogel increased as the initial dye concentration increased. This result

was due to the saturation of the active centers of the hydrogel. While the highest absorption capacity (28.6 mg/g) was reached with an initial dye concentration of 100 mg/L, the highest removal yield (99.6%) was reached with an initial dye concentration of 50 mg/L.

Determination of Kinetic Parameters. In order to determine the most suitable kinetic model, the sorption data were evaluated using four different kinetic models, i.e., pseudo first order, pseudo second order, intraparticle diffusion, and Endovich kinetic models. The parameters of the kinetic models, which were obtained based on the slopes and intercepts of the plotted graphs (Figure S2), are summarized in Table 3.

When we examined the data presented in Table 3, it was apparent that the calculated maximum sorption capacity values (q_c) using the pseudo second order kinetic model equation were closer to the experimentally-determined maximum sorption capacity (q_e), and the correlation coefficient was closer to
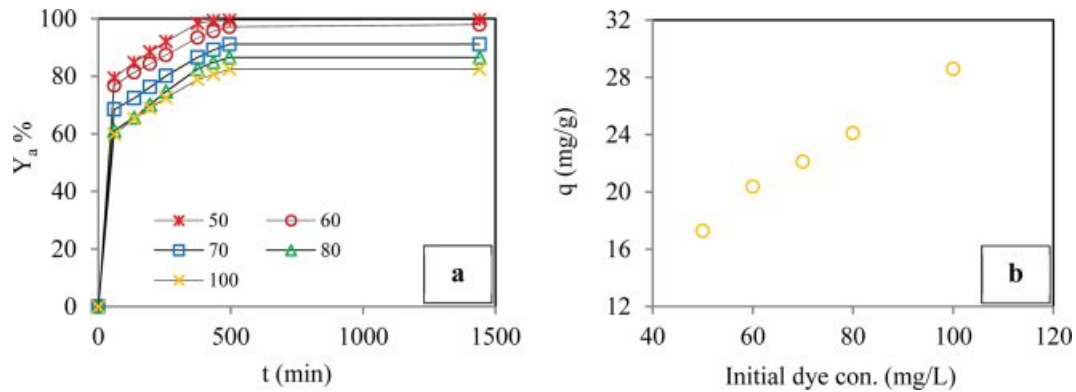
Figure 6. Effect of initial concentration of dye molecules on adsorption yield of dye (a); adsorption capacity of dye (b) (Conditions: pH of 6.5; temperature of 298 K; dye conc. of 50-100 ppm; contact time of 1440 min; agitation rate 180 rpm; cross-linker ratio of 1/4 mL/g; co-monomer ratio of 0/1 g/g).

Table 3. Parameters of the Kinetic Model for the Sorption of Dye Molecules

Model	Parameters	Values			
		298 K	308 K	318 K	328 K
Pseudo first-order kinetic model constants	R^2	0.9833	0.9877	0.9862	0.9857
	k_1 (1/min)	0.0106	0.0105	0.0111	0.0107
	q_{ec1} (mg/g)	21.151	48.139	67.640	50.154
	q_e (mg/g)	17.280	15.963	14.081	12.200
Pseudo second-order kinetic model constants	R^2	0.9966	0.9882	0.9779	0.9748
	k_2 (g/mg min)	0.0017	0.0007	0.0006	0.0006
	q_{ec2} (mg/g)	17.667	16.891	15.083	13.175
	q_e (mg/g)	17.280	15.963	14.081	12.200
	Error ratio	0.02	0.06	0.07	0.08
Enovich kinetic model constants	R^2	0.944	0.935	0.883	0.884
	α (mg/g min)	3.0807	2.058	1.689	1.383
	B (g/mg)	0.4043	0.452	0.512	0.597
Intra particle diffusion kinetic model constants	R^2	0.6335	0.7647	0.7518	0.781
	k_{id} (g/mg min$^{1/2}$)	0.3813	0.3765	0.339	0.2964
	C	5.8024	3.8021	3.069	2.4417

one. In contrast, the sorption capacities calculated using the so-called first order kinetic model were far different from the experimental data. In addition, we observed that the correlation coefficient was lower than that of the pseudo second order kinetic model. As a result, it was concluded that the pseudo second-order model mechanism was more suitable for modelling the sorption process. Using the equation for the pseudo second-order kinetic model, the maximum sorption capacities (q_c) for 298, 308, 318 and 328 K were calculated as 17.7, 16.9, 15.1, and 13.2 mg/g, respectively

The error ratios for 298, 308, 318, and 328 K were obtained as 0.02, 0.06, 0.07, and 0.08, respectively. The decreases in the

values of q_c and k_2 (g/mg.min) with temperature indicated that the dye molecules were adsorbed favorably by the gel at lower temperatures.

Similar results for the sorption of basic dye molecules onto different adsorbents have been reported in the literature, e.g., raw pine,[3] acid-treated pine cone powder,[3] pine cones,[9] chitosan-ethyl acrylate (Ch-g-Ea),[10] N, F co-doped, flower-like TiO$_2$ microspheres,[11] metal hydroxide sludge (MHS),[12] NaOH-pretreated rice husks,[13] milled sugarcane bagasse,[14] activated carbon,[15] graphene oxide,[15] multi-walled carbon nanotubes,[15] surfactant modified bentonite clay (organoclay),[21] copper nanowires loaded on activated carbon,[22] brick waste,[24] mixed

silica–alumina oxide,[25] pineapple (Ananas comosus) plant stems,[26] sawdust,[27] 3-allyloxy-2-hydroxy-1-propanesulfonic acid sodium salt.[28]

Figure S2(d) shows that the sorption process was divided into two parts and that the rate of sorption was different for the two parts. The first step, which might be attributable to external surface sorption, had a higher sorption rate than the second step at all of the temperatures. The second step could be viewed as a gradual sorption stage in which intraparticle diffusion is initiated, thereby decreasing the sorption rate in this step. The intraparticle diffusion stage controls and limits the rate of sorption. Table 3 provides the total sorption rate (k_{id}) as the average of the rates for the two steps for all of the temperatures. The kinetic calculations indicated that the values of k_{id} increased as the temperature increased.

Determination of Equilibrium Parameters. In order to determine the most suitable thermodynamic model, the sorption data at 298 K were evaluated using five different thermodynamic models, i.e., the Langmuir, Freundlich, Temkin, Boyd, and Dubinin-Radushkevich isotherm models. Parameters of the thermodynamic models, which were obtained using the slopes and intercepts of the plotted graphs (Figure S3), are summarized in Table 4.

Since the correlation coefficients for the Langmuir isotherm were closer to one (0.98), it was concluded that the Langmuir isotherm model was more suitable than the other models for modeling the process of removing the BB3 dye molecules. These results were in agreement with other studies, which also showed that the Langmuir model provided a good fit for the sorption of basic dye molecules. Similar sorption results have been reported in the literature.[9-11,13,15,18-20,22,24,25,29,34,39] Using the equation for the Langmuir isotherm model, the maximum monolayer sorption capacity (q_{max}) for 298 K was calculated as 28.3 mg/g. The numerical value of the R_L is important in the process of deciding either the shape of the isotherms is favorable, unfavorable, linear or irreversible. If $R_L=0$ it is irreversible, $0<R_L<1$ is favorable, $R_L=1$ is a liner, $R_L>1$ is unfavorable. The value calculated for RL for the Langmuir isotherm model, i.e., 0.008, was between 0 and 1. This result showed that the sorption process was suitable for the temperature and other conditions. The ratio, $1/n$, is the heterogeneity factor of sorption, and the calculated value of $1/n$ was to be 0.093. The calculated values of $1/n$ were less than 1.0 at all of the temperatures, which indicated that the dye molecules were adsorbed favorably and that their sorption was a chemically-driven process.

Table 4. Parameters of the Thermodynamic Model for the Sorption of Dye Molecules

Model	Parameters	Values
Langmuir isotherm constants	q_{max} (mg/g)	28.33
	K (L/mg)	1.213
	R_L	0.008
	R^2	0.982
Freundlich isotherm constants	n	10.78
	K_f (mg/g)	20.02
	R^2	0.892
Temkin isotherm constants	B (J/mol)	2.028
	K_T (L/mg)	21788.8
	R^2	0.838
D-R isotherm constants	Q_m (mg/g)	24.80
	β	0.00008
	E (J/mol)	79.06
	R^2	0.728

Parameters	Initial dye con. (mg/L)	Values
Boyd model constants		
$D_i \times 10^9$ (m^2/s)	50	3.067
	60	2.091
	70	2.063
	80	2.068
	100	2.072
B	50	0.00336
	60	0.00229
	70	0.00226
	80	0.00226
	100	0.00227
R^2	50	0.914
	60	0.745
	70	0.821
	80	0.892
	100	0.849

Characterization of Hydrogels Before and After Removal Process. The porosity of the hydrogel to be used in the removal process of BB3 dye molecules from the wastewater is important in terms of process efficiency. Therefore, in this study, we conducted SEM analyses of the hydrogel before and after removal process. SEM images were given in Figure 7.

Figure 7(a) clearly shows that the surface morphology of the gel before adsorption process was porous but the porosity of hydrogel was not homogeneous. Generally, it is known that such surfaces provide local mixing and enhanced adhesion in an aqueous solution, thereby increasing the sorption efficiency. After the sorption process, it was clearly observed in Figure
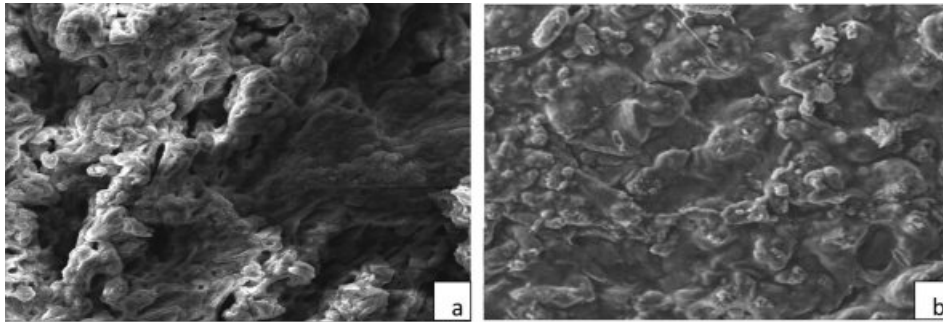
Figure 7. SEM images of the hydrogel before removal process (a); after removal process (b). ×1000.

Table 5. FTIR Assignments for the Hydrogel Before and After Removal Process

Absorption in wavenumber (cm⁻¹)		Assignments
Before removal process	After removal process	
3306	3341	The valence vibration corresponding to the NH groups from the crosslinking bridges,
2934	-	-CH- stretching vibrations. The CH_2 groups included in the macromolecular chains and crosslinking bridges.
-	2150	The steric strain effect on anhydride structure which may be formed by water dehydration.
1717	1717	The characteristic for carbonyl group (C=O) stretch for both amide ($CO-NH_2$) and carboxylic (COOH) groups absorption
1658-1613	1663	The stretching and deformation vibration of -C=O in polyacrylamide hydrogel and NH links from the amidic group
1453	1453	C-N stretching vibrations. Cyano group (C-N) on the chains of PAAm give absorption band
1323-1148	1323-1151	Sorption bands assigned to the deformation vibrations of the -C-N- links and CH_2 groups

7(b) that the pores had disappeared and a rough and not porous surface was formed. As a results, it was concluded that the surface of hydrogel has a more porous surface the before sorption process, ie. the pores of the hydrogel were filled by BB3 dye molecules.

In addition, it is well known when the sorption process was used to remove BB3 dye molecules from the wastewater, the functional groups found in the active centers of the sorbent

were highly related. These functional groups may be joined with dye molecules. Thus, dye molecules can be removed from the wastewater. Therefore, in this study, we conducted FTIR analyses of the hydrogel before and after sorption. Figure S4 shows the FTIR spectrum, indicating the presence of C=O bond, C-N bonds, C=C bond, and C-H bond. The functional groups, vibrational frequency and their assignment that were obtained from the FTIR spectrum were summarized in Table 5. Sorption band attribution was made in agreement with the values given in the literature.[32,40,41]

Regeneration Efficiency of Hydrogel. The success of the desorption process depends largely on the sorbent type and the sorption mechanism. These two parameters influence the selection of the appropriate washing solution. In addition, the washing solution should not damage the sorbent, should be low cost, environmentally friendly and effective.[42] In this study, 0.1 M HCl washing solution was used. The sorption/desorption cycle was repeated three times. Table 6 shows that desorption efficiencies of AAm-based hydrogels were found to be above 90%. The efficiency of desorption was taken into account as the ratio of the amount of sorbet to the amount of desorbed. During the desorption process, the hydrogel has not undergone any deformation in shape, because the acid concentration was low (0.1 M). Further, dissolution or disintegration was not observed. Therefore, the gel protected its physical stability under these desorption conditions. Figure 8 shows, the photographs of the hydrogel before desorption process (a) and after desorption process (b).

Comparison. In order to decide the applicability of the sorption process, it was very important to determine the kinetic and equilibrium parameters, to calculate the maximum sorption capacity of the adsorbent, and to compare the value obtained with the literature. For this purpose, the sorption capacities that were obtained in previous studies of the removal of the dye molecules were summarized in Table S4.

Table 6. Desorption Characteristics of BB3 dye Sorbed on Acrylamide Based Hydrogel

C_0 (ppm)	C_e (ppm)	Y_a %	C_a (ppm)	C_s (ppm)	(C_a-C_s) (ppm)	D_e %
50.00	0.16	99.68	49.84	4.98	44.86	90.00
60.00	0.85	98.58	59.15	4.81	54.34	91.87
70.00	6.27	91.04	63.73	4.41	59.32	93.07
80.00	10.75	86.56	69.25	4.78	64.47	93.10
100.0	16.53	83.47	83.47	5.120	78.35	93.86

Desorption conditions: temperature of 298 K; contact time of 1440 min; agitation rate 180 rpm; washing solution: 0.1M HCl.
Hydrogel composition: cross-linker ratio of 1/4 mL/g; comonomer ratio of 0/1 g/g.
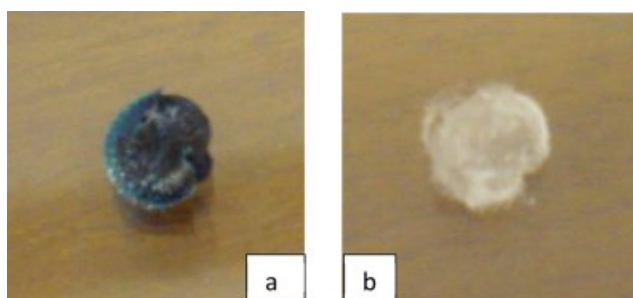
Figure 8. Photograph of the hydrogel before desorption process (a); after desorption process (b).

Conclusions

In this research paper, the sorption properties of the BB$_3$ dye molecules to the AAm-based hydrophilic gel structure were evaluated in different gel compositions (co-monomer ratio, cross-linker ratio) and sorption conditions (initial dye concentration, temperature of the solution and contact time, initial pH of the solution). First, AAm-based hydrogels were synthesized using chemical polymerization and characterized. Then, the temperature-dependent equilibrium swelling ratios of the hydrophilic gels in water were determined with gravimetric methods. Subsequently, the sorption experiments were conducted at various conditions.

· The experimental results indicated that the water sorption capacity of the gel decreased as the ratio of the co-monomer of the hydrogel increased.

· Until the cross-linking density reaches the critical value (EGDM/monomer (v/w: mL/g) ratio of 0.25/1), the potential swelling ratio of the gel increased, after this critical value, the increase in the cross-linking density led to a decrease in the water sorption capacity.

· The temperature at which the AAm-based gel films absorbed the maximum amount of water was determined to be 308 K.

· The water sorption capacity of gel at the optimum conditions (308 K; EGDM/monomer (v/w: mL/g) ratio of 0.25/1; NIPAm/monomer (w/w: g/g):0/1) were determined to be 14 g_{water}/g_{gel}, respectively.

· The experimental results showed that the removal yield of BB$_3$ increased due to the increased contact time. The trends observed for the temperature and initial dye concentration of the solution were the opposite of this.

· The optimum values of the co-monomer ratio, cross-linker ratio, temperature, pH, contact time, and the initial concentration of the BB3 dye molecules were NIPAm/monomer (w/w:g/g): 0/1; EGDM/monomer (v/w:mL/g): 0.25/1; 298 K; 6.5 ± 0.02; 440 min; and 50 ppm, respectively. The sorption yield of dye molecules and the sorption capacity (q_e) of the hydrogel at the optimum conditions were determined to be 99% and 17.3 mg/g, respectively.

· When the parameters obtained using four different sorption kinetic models were examined, it was concluded that the pseudo second-order kinetic model was described by the adsorption data very well. Using the equation for the pseudo-second kinetic model, the maximum sorption capacities (q_c) for 298, 308, 318, and 328 K were calculated 17.7, 16.9, 15.1 and 13.2 mg/g, respectively. The decreases in the values of q_c and k_2 (g/mg.min) with temperature indicated that the dye molecules were adsorbed favorably by the gel at lower temperatures.

· When the parameters obtained using five different sorption isotherm models were examined, it was determined that the Langmuir was more suitable for isotherm the process. The maximum sorption capacity was calculated as 28.3 mg/g using the Langmuir isotherm. Since the R_L was between 0 and 1, it was determined that the sorption process was favorable.

Supporting Information: The detailed information about experimental procedure for the sorption application of Basic blue 3 dye molecules was contained in the supporting information document. Sorbent composition, sorption conditions, kinetic and thermodynamic model equations, FTIR spectrum of sorbent (before and after sorption) and the summary of the literature related to the sorption of basic dye molecules were presented at http://journal.polymer-korea.or.kr.

References

1. M. T. Yagub, T. K. Sen, S. Afroze, and H. M. Ang, *Colloid Interface Sci*., **209**, 172 (2014).
2. K. S. Bharathi and S. T. Ramesh, *Appl. Water Sci.*, **3**, 773 (2018).
3. S. Dawood and T. K. Sen, *Water Res.*, **46**, 1933 (2012).
4. R. K. Vital, K. V. N. Saibaba, K. B. Shaik, and R. Gopinath, *J. Bioremediat. Biodegrad.*, **7**, 1 (2016).
5. M. Kaykhaii, M. Sasani, and S. Marghzari, *Chem. Mater. Eng.*, **6**, 31 (2018).
6. S. Sivamani and B. L. Grace, *I.J.BST*, **2**, 47 (2009).
7. M. Chincholi, P. Sagwekar, C. Nagaria, S. Kulkarni, and S. Dhokpande, *IJSETR*, **3**, 835 (2014).
8. A. R. Warade, R. W. Gaikwad, R. S. Sapkal, and V. S. Sapkal, *IJARIIE*, **2**, 3851 (2016).
9. A. S. Mohammadi, M. Sardara, A. Mohammadib, F. Azimia, and N. Nurieh, *Archives of Hygiene Sciences*, **2**, 158 (2013).
10. M. Sadeghi-Kiakhani, M. Arami, and K. Gharanjig, *J. Environ. Chem. Eng.*, **1**, 406 (2013).
11. Y. Jiang, Y. Luo, F. Zhang, L. Guo, and L. Ni, *Appl. Surf. Sci.*, **273**, 448 (2013).
12. M. Attallah, I. Ahmed, and M. M. Hamed, *Environ. Sci. Pollut. Res.*, **20**, 1106 (2013).
13. L. Lin, S. R. Zhai, Z. Y. Xiao, Y. Song, Q. D. An, and X. W. Song, *Bioresour. Technol.*, **136**, 437 (2013).
14. Z. Zhang, I. M. O'Hara, G. A. Kent, and W. O. S. Doherty, *Ind. Crop. Prod.*, **42**, 41 (2013).
15. Y. Li, Q. Du, T. Liu, X. Peng, J. Wang, J. Sun, Y. Wang, S. Wu, Z. Wang, Y. Xia, and L. Xia, *Chem. Eng. Res. Design*, **91**, 361 (2013).
16. G. L. Dotto, J. M. Moura, T. R. S. Cadaval, and L. A. A. Pinto, *Chem. Eng. J.*, **214**, 8 (2013).
17. B. A. Sadler and L. Metals, *Removal of Methylene Blue from Aqueous Solution Using a Novel Red Mud Mixed with Cement*, John Wiley & Sons Inc., Hoboken, New Jersey, p 1-133 (2013).
18. M. Roosta, M. Ghaedi, N. Shokri, A. Daneshfar, R. Sahraei, and A. Asghari, *Spectrochim. Acta. A Mol. Biomol. Spectrosc.*, **118** 55 (2014).
19. Z. Zhou, S. Lin, T. Yue, and T. C. Lee, *J. Food Eng.*, **126**, 133 (2014).
20. P. F. Wang, M. H. Cao, C. Wang, Y. H. Ao, J. Hou, and J. Qian, *J. Appl. Surface Sci.,* **290**, 116 (2014).
21. T. S. Anirudhan and M. Ramachandran, *Process Saf. Environ. Prot.*, **95**, 215 (2015).
22. M. Ghaedi, E. Shojaeipour, A. M. Ghaedi, and R. Sahraei, *Spectrochim. Acta A Mol. Biomol. Spectrosc.*, **142**, 135 (2015).
23. Y. Premkumar and K. Vijayaraghavan, *Sep. Sci. Technol.*, **50**, 1439 (2015).
24. F. Kooli, L. Yan, R. Al-Faze, and A. Al-Sehimi, *Arab. J. Chem.*, **8**, 333 (2015).
25. M. Wawrzkiewicz, M. Wiśniewska, V. M. Gun'ko, I. Vladimir, and V. I. Zarko, *Powder Technol.*, **278**, 306 (2015).
26. S. L. Chan, Y. P. Tana, A. H. Abdullah, and S. T. Ong, *J. Taiwan Institute Chem. Eng.*, **61**, 306 (2016).
27. S. Banerjee and M. Chattopadhyaya, *Arab. J. Chem.*, **10**, 1629 (2017).
28. A. G. Ibrahim, F. A. Hai, H. Abd El-Wahab, and H. Aboelanin, *Adv. Polym. Technol.*, **37**, 3561 (2018).
29. S. Kang, Y. Zhao, W. Wang, T. Zhang, T. Chen, H. Yi, F. Rao, and S. Song, *Appl. Surf. Sci.*, **448**, 203 (2018).
30. S. Sudarsan, D. S. Franklin, M. Sakthivel, G. Chitra, T. B. Sridharan, and S. Guhanathan, *J. Polym. Environ.*, **26**, 3773 (2018).
31. D. Saraydın, Y. Işıkver, and E. Karadağ, *Polym. Eng. Sci.*, **58**, 310 (2018).
32. T. E. Dudu, D. Alpaslan, and Y. Uzun, *Int. J. Environ. Res.*, **11**, 557 (2017).
33. K. Bello, B. K. Sarojini, B. N. Anjali, and R. K. Byrappa, *Carbohydr. Polym.*, **181**, 605 (2018).
34. N. Mohammed, N. Grishkewich, R. M. Berry, and K. C. Tam, *Cellulose*, **22**, 3725 (2015).
35. E. Makhado, S. Pandey, P. N. Nomngongo, and J. Ramontja, *J. Colloid Interface Sci.*, **513**, 700 (2018).
36. W. Wang, Y. Zhao, H. Bai, T. Zhang, V. Ibarra-Galvan, and S. Song, *Carbohydr. Polym.*, **198**, 518 (2018).
37. F. A. Ngwabebhoh, M. Gazi, and A. A. Oladipo, *Chem. Eng. Res. Design*, **112**, 274 (2016).
38. V. V. Panic and S. J. Velickovic, *Sep. Purif. Technol.*, **122**, 384 (2014).
39. S. Ghorai, A. Sarkar, M. Raoufi, A. B. Panda, H. Schönherr, and S. Pal, *ACS Appl. Mater. Interfaces*, **6**, 4766 (2014).
40. R. Akkaya, and U. Ulusoy, *Hacettepe J. Biol. Chem.*, **39**, 359 (2011).
41. A. M. Dumitrescu, G. Lisa, A. R. Iordan, F. Tudorache, I. Petrila, A. I. Borhan, M. N. Palamaru, C. Mihailescu, L. Leontie, and C. Munteanu, *Mater. Chem. Phys.*, **156**, 170 (2015).
42. K. Vijayaraghavan and Y. S. Yun, *Biotechnol. Adv.*, **26**, 266 (2008).